



Photodeposition of Pd nanoparticles on ZnIn₂S₄ for efficient alkylation of amines and ketones' α-H with alcohols under visible light

Bingqing Wang, Zirong Deng, Xianzhi Fu, Chao Xu*, Zhaohui Li*

Research Institute of Photocatalysis, State Key Laboratory of Photocatalysis on Energy and Environment, College of Chemistry, Fuzhou University, Fuzhou 350116, PR China



ARTICLE INFO

Keywords:
Photocatalytic
Pd-ZnIn₂S₄
Alkylation reaction
Alcohols
Hydrogen auto-transfer

ABSTRACT

Pd nanoparticles with a small size of ca. 6 nm were deposited on the surface of ZnIn₂S₄ via photoreduction of Pd (CH₃CN)₂Cl₂ over ZnIn₂S₄ under visible light. The resultant Pd-ZnIn₂S₄ nanocomposites were fully characterized and their catalytic performance for light induced N-alkylation of amines and α-H alkylation of ketones with alcohols were investigated. It was found that Pd-ZnIn₂S₄ nanocomposites show superior catalytic activity for the alkylation reactions via a successful coupling of the photocatalytic dehydrogenation of alcohols over ZnIn₂S₄ with Pd-based hydrogenation. An optimum performance was realized over 0.5 wt% Pd-ZnIn₂S₄ nanocomposites by synchronization of the rates of different reaction steps in the tandem alkylation reaction. Ascribed to the small sized Pd nanoparticles, which provide more active unsaturated Pd atoms, Pd-ZnIn₂S₄ nanocomposites obtained via photoreduction show superior performance as compared to Pd/ZnIn₂S₄ obtained via a chemical reduction using NaBH₄. This study provides an efficient way to realize a highly efficient and stable alkylation of amines and α-H of ketones with alcohols under visible light. This study also highlights the great potential of construction of multifunctional catalysts for light induced organic syntheses.

1. Introduction

An effective synthetic strategy in construction of C–N and C–C bonds, one of the most important tasks in organic synthesis, is to react N– and C– containing reagents with alkylating agents [1,2]. As compared with traditional alkylating agents like alkyl halides, alkyl tosylates, alkyl triflates and alkyl sulfonates etc., which contains easily leaving groups [3], the use of nontoxic and bulk available alcohols as alkylating agents is more attractive since such a reaction has high atom efficiency and produces water as the only byproduct, yet it is more challenging [4]. Ever since the pioneering work by Watanabe and Grigg reported the use of alcohols for the N-alkylation of amines [5,6], extensive research interest has been devoted to the direct use of alcohols in the alkylating reactions in the past two decades. A variety of homogeneous catalysts, mostly noble metal based complexes, as well as some metal nanoparticle doped heterogeneous catalysts, have been developed for alcohols-involved alkylating reactions [7–10]. Usually the homogeneous systems suffer from limited reusability and the indispensable use of the co-catalysts, while most of the heterogeneous systems are carried out in elevated temperature, in which over-alkylation sometimes occurs. The development of efficient heterogeneous catalytic systems for alcohols-involved alkylating reactions under mild

conditions is highly desirable.

Based on previous studies, transition metal catalyzed alcohols-involved alkylation reactions follows a hydrogen auto-transfer mechanism containing three consecutive catalytic steps: dehydrogenation of alcohols to aldehydes, condensation between aldehydes and nucleophilic reagents (amines or ketones, etc.) to form corresponding intermediates, followed by hydrogenation of the intermediates to form the targeted alkylated products [11–13]. Multifunctional catalysts containing different catalytically active sites for these consecutive steps respectively can realize an efficient alkylation reaction in one pot. Currently, with an aim of developing renewable energy based processes, researchers are paying particular interest to light induced organic syntheses [14–18]. As a result, a variety of multifunctional MNPs/photocatalyst (MNPs = metal nanoparticles) nanocomposites, including MNPs/TiO₂ (M = Pd, Au, Cu-Mo alloy) and M@MIL-100(Fe) (M = Pd and AuPd), have been applied for N-alkylation reactions by successful coupling of photocatalytic dehydrogenation of alcohols to form aldehydes with the MNPs-based hydrogenation [19–24].

Hexagonal ZnIn₂S₄ is a stable semiconductor chalcogenide with a band gap corresponding to the visible light absorption [25]. Endowed with suitable band position, ZnIn₂S₄ has been extensively studied for photocatalytic H₂ evolution, degradation of organic dyes as well as

* Corresponding authors.

E-mail addresses: cxu@fzu.edu.cn (C. Xu), zhaohuili1969@yahoo.com (Z. Li).

organic transformations [25–31]. In particular, since the top of the valence band of ZnIn_2S_4 locates at 1.37 eV vs NHE, the moderate oxidation potential of the holes prevents the synthesized organic compounds from being oxidized in an uncontrollable manner, which makes ZnIn_2S_4 to be promising photocatalyst for organic transformations. Actually, the photocatalytic oxidation of benzyl alcohol and amines over ZnIn_2S_4 have already been reported [32,33]. It is therefore anticipated that the photocatalytic dehydrogenation of alcohols to form aldehydes over ZnIn_2S_4 can be coupled with Pd-based hydrogenation to realize the tandem alkylation reactions between alcohols and nucleophilic agents. For this purpose, Pd nanoparticles with small size should be deposited on the surface of ZnIn_2S_4 since it is generally accepted that smaller Pd nanoparticles usually contain more active unsaturated Pd atoms. In the alkylation reactions, these active Pd sites abstract hydrogen from the alcohols to form Pd-H, which acts as the active species for the hydrogenation reaction [19].

Herein we reported the deposition of small sized Pd nanoparticles (ca. 6 nm) on the surface of ZnIn_2S_4 via a photoreduction process and the resultant Pd- ZnIn_2S_4 nanocomposites were used for light induced alkylation of amines and α -H of ketone. It was found that Pd- ZnIn_2S_4 nanocomposites are active for the alkylation reaction under visible light via a successful coupling of the photocatalytic dehydrogenation of alcohols over ZnIn_2S_4 with Pd-based hydrogenation, with an optimum performance observed over 0.5 wt% Pd- ZnIn_2S_4 nanocomposites. This work demonstrates an efficient way to realize the alkylation of amines and α -H of ketones and also highlights the great potential of construction of multifunctional catalysts for light induced organic syntheses.

2. Experimental

2.1. Preparations

All the reagents were commercial available and used without further purifications. Bis(acetonitrile)dichloropalladium(II) ($\text{Pd}(\text{CH}_3\text{CN})_2\text{Cl}_2$) was prepared by refluxing PdCl_2 in CH_3CN according to literature [34]. ZnIn_2S_4 were synthesized from $\text{ZnCl}_2\cdot 6\text{H}_2\text{O}$ and $\text{InCl}_3\cdot 4.5\text{H}_2\text{O}$ in a mixed solvent of *N,N*-Dimethylformamide (DMF) and ethylene glycol (EG) via a solvothermal process according to our previous report [25]. Pd nanoparticles were loaded on the surface of ZnIn_2S_4 via a photoreduction process and were denoted as x wt% Pd- ZnIn_2S_4 , in which x was referred to the amount of Pd in the nanocomposites ($x = 0.3, 0.5, 1.0$). Take 0.5 wt% Pd- ZnIn_2S_4 for example, a mixture of ZnIn_2S_4 (200 mg) and $\text{Pd}(\text{CH}_3\text{CN})_2\text{Cl}_2$ (1.63 mg) was dispersed in a mixed solution containing 0.5 ml TEOA and 3.5 ml acetonitrile (CH_3CN). After degassed, the suspension was irradiated with a 300 W Xe lamp for 2 h. The resultant product was washed with ethanol and dried overnight at 60 °C in oven. For comparison, a chemical reduction process using NaBH_4 as the reducing agent was also used in the preparation of 0.5 wt% Pd dispersed on ZnIn_2S_4 (denoted as 0.5 wt% Pd/ ZnIn_2S_4).

2.2. Characterizations

The X-ray diffraction (XRD) patterns of the as-obtained products were carried out on a D8 Advance X-ray diffractometer (Bruker, Germany) using $\text{Cu K}\alpha$ ($\lambda = 1.5406 \text{ \AA}$) radiation at a voltage of 40 kV and 40 mA. XRD patterns were scanned over the angular range of 10–70° (2θ) with a step size of 0.02°. X-ray photoelectron spectroscopy (XPS) measurements were performed on a PHI Quantum 2000 XPS system (PHI, USA) with a monochromatic $\text{Al K}\alpha$ source and a charge neutralizer. All the binding energies were referenced to the C1s peak at 284.6 eV of the surface adventitious carbon. The transmission electron microscopy (TEM) and high resolution TEM (HRTEM) images were measured by JEOL model JEM 2010 EX instrument at an accelerating voltage of 200 kV. UV-visible diffuse reflectance spectra (UV-DRS) of

the powders were obtained with the BaSO_4 used as a reflectance standard in the UV-visible diffuse reflectance experiment.

2.3. Catalytic reactions

The light induced alkylation reactions were carried out in a sealed reaction tube with a 300 W Xe arc lamp (Beijing Perfect light, PLS-SXE300c). For the N-alkylation reactions, the catalyst (10 mg) and amines (0.2 mmol) were suspended in a solvent containing excess benzyl alcohol (2 mL). Before the reaction, the suspension was degassed and saturated with N_2 to remove any dissolved O_2 . The reaction was performed under irradiation with a 300 W Xe lamp equipped with a UV-cut filter to remove all irradiation with wavelengths less than 420 nm and an IR-cut filter to remove all irradiation with wavelengths greater than 800 nm. After the reaction, the resultant suspension was filtered through a porous membrane (20 μm in diameter) and the filtrate was analyzed by GC-MS and GC-FID (Shimadzu GC-2014) equipped with an HP-5 capillary column.

For the α -H alkylation of ketones, the catalyst (10 mg), acetophenone (0.2 mmol) and Cs_2CO_3 (0.1 mmol) were suspended in a solvent containing excess benzyl alcohol (2 mL).

3. Results and discussion

Hexagonal ZnIn_2S_4 was obtained solvothermally from ZnCl_2 and InCl_3 in a mixed solution of DMF and EG following the previously reported method [25]. Pd- ZnIn_2S_4 nanocomposites with different amount of Pd were prepared from the as-obtained ZnIn_2S_4 and $\text{Pd}(\text{CH}_3\text{CN})_2\text{Cl}_2$ via a photoreduction process in the presence of TEOA. It was found that the color of the suspension changed gradually from the original yellow to deep brown during the light irradiation. The XRD patterns of the as-obtained product not only shows similar diffraction patterns, but also comparable intensity and full width at half maxima (FWHM) of the characteristic diffraction peaks, as that of bare ZnIn_2S_4 , indicating that the integrity and crystallinity of ZnIn_2S_4 was maintained during the photoreduction process (Fig. 1). Although no characteristic diffraction peaks corresponding to metallic Pd were observed, probably due to the low loading amount and their homogeneous dispersion in the sample, the XPS spectra of 0.5 wt% Pd- ZnIn_2S_4 nanocomposites confirms the presence of metallic Pd by showing two peaks at binding energy of 335.0 and 340.2 eV, assignable to $\text{Pd}^\circ 3\text{d}_{5/2}$ and $\text{Pd}^\circ 3\text{d}_{3/2}$, respectively (Fig. 2) [35]. The successful deposition of small-sized Pd nanoparticles is also evidenced from the TEM images of Pd- ZnIn_2S_4 nanocomposites (Fig. 3). The TEM image of 0.5 wt% Pd- ZnIn_2S_4 nanocomposites shows that it consists of flower-like microspheres with an average size of 6.0 μm, similar to that of bare ZnIn_2S_4 (Fig. 3a). An enlarged TEM image shows that each microsphere is comprised of large numbers of interwoven ultrathin nanosheets, with small nanoparticles in a size of ca. 6.0 nm evenly deposited on the surface of these ultrathin nanosheets

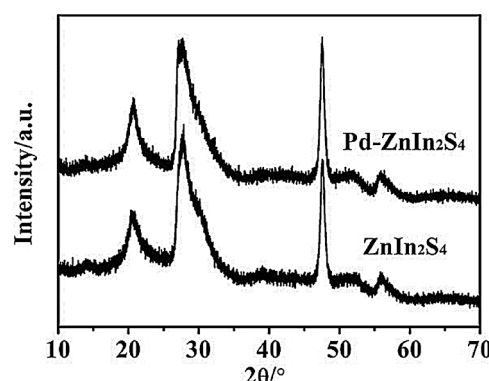


Fig. 1. XRD patterns of ZnIn_2S_4 and 0.5 wt% Pd- ZnIn_2S_4 .

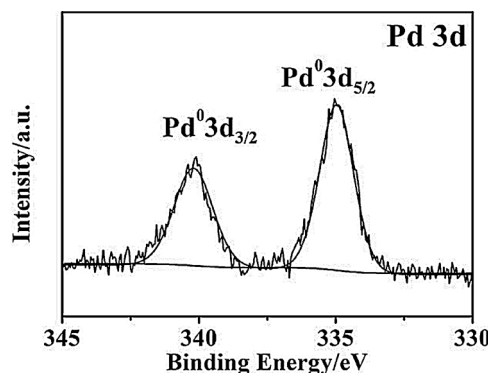
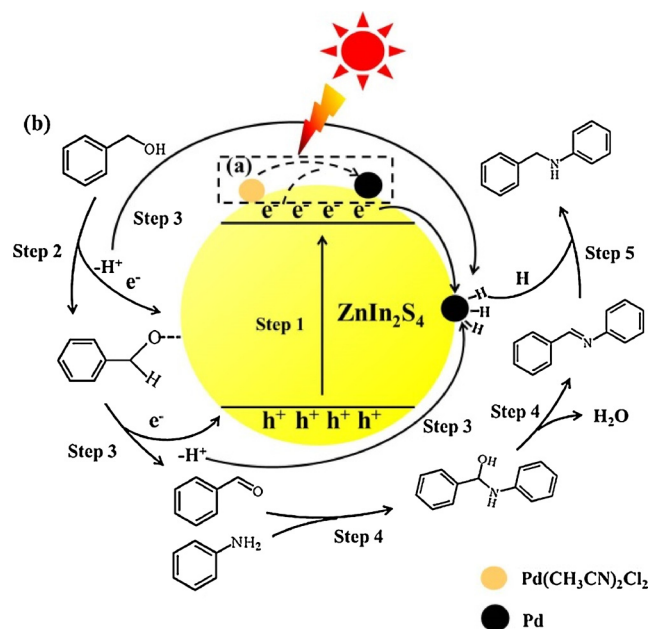


Fig. 2. XPS spectra of 0.5 wt% Pd-ZnIn₂S₄ in Pd 3d region.

(Fig. 3b). In addition to lattice fringes of 0.322 nm, which belongs to (102) crystal plane of hexagonal ZnIn₂S₄ [36], the HRTEM image also shows clear lattice fringes of 0.224 nm, matches that of the (111) plane of face-centered cubic Pd (Fig. 3c) [23].

All these characterizations demonstrate that robust Pd-ZnIn₂S₄ nanocomposites with small-sized Pd nanoparticles deposited on ZnIn₂S₄ microspheres has been successfully obtained via the photoreduction process. It is proposed that the first step in the deposition of Pd nanoparticles on ZnIn₂S₄ is the adsorption of the positive Pd precursor [Pd(CH₃CN)₂]²⁺ on the negative charged S planes of ZnIn₂S₄ [37], as evidenced from a quick darken of yellow ZnIn₂S₄ when Pd(CH₃CN)₂Cl₂ was added into the suspension of ZnIn₂S₄. Since the bottom of the conduction band of hexagonal ZnIn₂S₄ (-1.1 V vs NHE) is negative than the reduction potential of Pd(CH₃CN)₂²⁺/Pd (0.24 V vs NHE, Supporting information Fig. S1), the photogenerated electrons on hexagonal ZnIn₂S₄ can reduce the surface adsorbed [Pd(CH₃CN)₂]²⁺ to form Pd nanoparticles, while the photogenerated holes left on the valence band can react with TEOA, the sacrificial agent to complete the photocatalytic cycle (Scheme 1a). The adsorption of [Pd(CH₃CN)₂]²⁺ on the surface of ZnIn₂S₄ is the prerequisite for the formation of Pd-ZnIn₂S₄ nanocomposites with strong interaction between Pd nanoparticles and hexagonal ZnIn₂S₄, while the photoreduction can ensure a moderate reaction condition to produce the evenly deposited Pd with small size. As compared with bare ZnIn₂S₄, the UV-vis DRS spectrum of 0.5 wt% Pd-ZnIn₂S₄ nanocomposites shows slightly enhanced absorption in the 200–600 nm region, due to the introduction of Pd nanoparticles (Fig. 4).

To study the catalytic performance of the as-prepared Pd-ZnIn₂S₄ nanocomposites for alkylation reactions with alcohols under visible light irradiation, the reaction between benzyl alcohol (1a) and aniline (2a) was first chosen as a model reaction. The reaction was initially carried out in excess benzyl alcohol as solvent over 0.5 wt% Pd-ZnIn₂S₄ nanocomposites. It was found that 47% of aniline was converted after irradiated for 18 h, with a selectivity of 31% to the desired alkylation product N-benzylideneaniline (3a). N-benzylideneaniline (3b) and benzaldehyde as the intermediates are the main byproducts, but no over-



Scheme 1. (a) Illustration of the deposition of Pd nanoparticles over ZnIn₂S₄ via photoreduction and (b) proposed mechanism for N-alkylation of aniline with benzyl alcohol via hydrogen transfer process over Pd-ZnIn₂S₄.

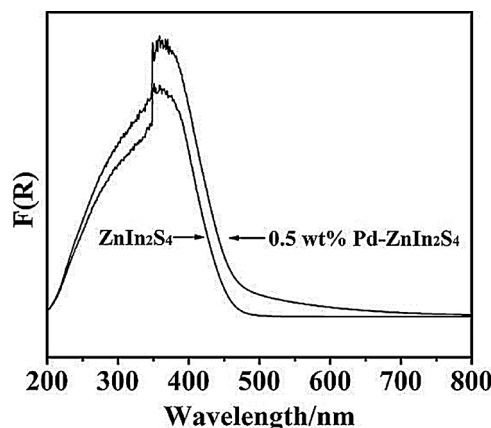


Fig. 4. UV-vis spectra of ZnIn₂S₄ and 0.5 wt% Pd-ZnIn₂S₄.

alkylated tertiary amine was detected (Table 1, entry 1). Only 9% of aniline was converted over bare ZnIn₂S₄ under similar condition, with the main product obtained to be 3b (7%) (Table 1, entry 2), indicating that Pd is essential for the transformation of the intermediate 3b to the desired alkylation product 3a. Almost negligible aniline was converted either in absence of 0.5 wt% Pd-ZnIn₂S₄ or without visible light (Table 1, entries 3–4). The filtrate reaction revealed that no further

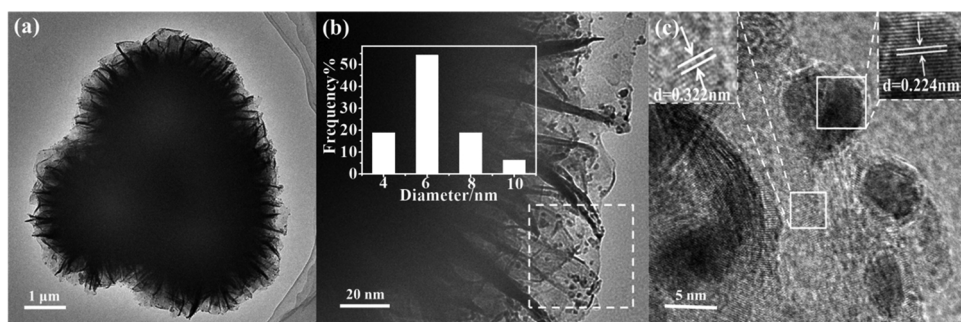


Fig. 3. (a) TEM image; (b) Enlarged TEM image (inset shows the size distribution of Pd nanoparticles); (c) HRTEM image of 0.5 wt% Pd-ZnIn₂S₄.

Table 1Light induced catalytic performance for N-alkylation of aniline with benzyl alcohol over Pd-ZnIn₂S₄ under different conditions.

Entry	Catalyst	Solvent	Aniline conv. /%	Yield /%		Aldehyde / μmol
				3a	3b	
1	0.5 wt%Pd-ZnIn ₂ S ₄	benzyl alcohol	47	31	15	41
2	ZnIn ₂ S ₄	benzyl alcohol	9	2	7	8
3 ^a	-	benzyl alcohol	- ^c	- ^c	- ^c	- ^c
4 ^b	0.5 wt%Pd-ZnIn ₂ S ₄	benzyl alcohol	- ^c	- ^c	- ^c	- ^c
5 ^d	0.5 wt%Pd-ZnIn ₂ S ₄	benzyl alcohol	50	31	19	41
6	0.5 wt%Pd-ZnIn ₂ S ₄	DMF/benzyl alcohol (1:1)	48	14	42	52
7	0.5 wt%Pd-ZnIn ₂ S ₄	H ₂ O/benzyl alcohol (1:1)	3	- ^c	3	6
8	0.5 wt%Pd-ZnIn ₂ S ₄	toluene/benzyl alcohol (1:1)	41	8	32	49
9	0.5 wt%Pd-ZnIn ₂ S ₄	CH ₃ CN/benzyl alcohol (1:1)	57	24	33	28
10	0.5 wt%Pd-ZnIn ₂ S ₄	CH ₃ CN/benzyl alcohol (1:5)	70	47	20	69
11	0.5 wt%Pd-ZnIn ₂ S ₄	CH ₃ CN/benzyl alcohol (1:9)	82	73	9	93
12 ^e	0.5 wt%Pd-ZnIn ₂ S ₄	CH ₃ CN/benzyl alcohol (1:9)	99	93	5	132
13	0.3 wt%Pd-ZnIn ₂ S ₄	CH ₃ CN/benzyl alcohol (1:9)	84	51	32	98
14	1.0 wt%Pd-ZnIn ₂ S ₄	CH ₃ CN/benzyl alcohol (1:9)	69	41	16	74
15 ^f	0.5 wt%Pd-ZnIn ₂ S ₄	CH ₃ CN/benzyl alcohol (1:9)	78	55	21	78

Reaction conditions: aniline (0.2 mmol), catalyst (10 mg), solvent (2 mL), N₂, irradiated for 18 h. ^a No catalyst. ^b Without light irradiation. ^c refers to no products or negligible products detected. ^d The catalyst was filtered after being irradiated for 18 h. ^e Irradiated for 24 h. ^f Pd/ZnIn₂S₄ used as catalyst.

reaction occurred after 0.5 wt% Pd-ZnIn₂S₄ was removed from the reaction system after reacting for 18 h (Table 1, entry 5). These results demonstrated that the N-alkylation of aniline with benzyl alcohol is truly induced by visible light induced catalysis over Pd-ZnIn₂S₄ nanocomposites.

To study the effect of the solvents on the catalytic performance, a mixed solvent containing CH₃CN, DMF, H₂O and toluene respectively, in 1:1 vol ratio to benzyl alcohol, were used for the N-alkylation of aniline (Table 1, entries 6–9). Among all the four solvents investigated, CH₃CN was found to be the best solvent by showing a slightly enhanced conversion of aniline at 57%, but a relatively lower yield of 24% to the desired 3a after irradiated for 18 h. This indicates that the introduction of CH₃CN improves the aniline conversion, yet it is disadvantage for the transformation of 3b to the desired alkylating product 3a. The decrease of the ratio of CH₃CN to benzyl alcohol in the mixed solvent led to an improved aniline conversion as well as enhanced yield to the desired 3a (Table 1, entries 10–11). An optimum aniline conversion of 82% and a yield of 73% to the desired 3a can be achieved after being irradiated for 18 h in a mixed medium with CH₃CN and benzyl alcohol in a volume ratio of 1: 9. A prolonged reaction time to 24 h in this system led to an almost quantitative transformation of aniline (99%) with an superior yield of 93% to 3a (Table 1, entry 12). In addition, Pd-ZnIn₂S₄ nanocomposites showed high stability for the light induced N-alkylation of aniline reaction. No obvious loss of the activity was observed after three cycling tests and the catalyst after three runs showed similar XRD patterns (Fig. 5 and Supporting Fig. S2a). No re-construction of Pd

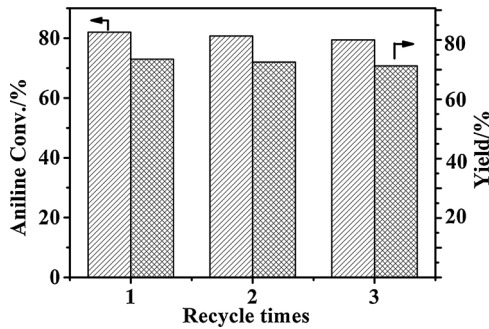


Fig. 5. Cycling of 0.5 wt% Pd-ZnIn₂S₄ for the N-alkylation of aniline with benzyl alcohol under visible-light irradiation.

nano-particles occurs during the reaction since Pd nanoparticles after the reaction show almost unchanged morphology as evidenced from the TEM image (Supporting information Fig. S2b).

The time-dependent conversion of aniline and the formation of the products over 0.5 wt% Pd-ZnIn₂S₄ in a mixed solvent of CH₃CN: benzyl alcohol (1:9) was shown in Fig. 6. It was found that the amount of the desired alkylating product 3a and benzaldehyde increased with the irradiation time. However, the amount of 3b increased first, but decreased after 3 h, suggesting the transformation of 3b to 3a during the reaction process. This result confirms that the reaction between aniline and benzyl alcohol to produce 3a over irradiated Pd-ZnIn₂S₄ nanocomposites also proceeds through 3b as an intermediate, in consistent with our previous studies on the N-alkylation of amine over Pd@MIL-100(Fe) [23].

The mechanism for the light induced N-alkylation of aniline by benzyl alcohol over Pd-ZnIn₂S₄ can therefore be proposed (Scheme 1b). ZnIn₂S₄ can be excited by visible light to generate electrons and holes. The photogenerated electrons are transferred from ZnIn₂S₄ to Pd nanoparticles to form electron-rich Pd species (step 1) [38], while the surface adsorbed benzyl alcohol reacts with the photogenerated holes, leading to the formation of an alkoxide intermediate (step 2). The further cleavage of the C–H bond in the alkoxide intermediate leads to the formation of benzaldehyde, with the hydrogen transferred to the

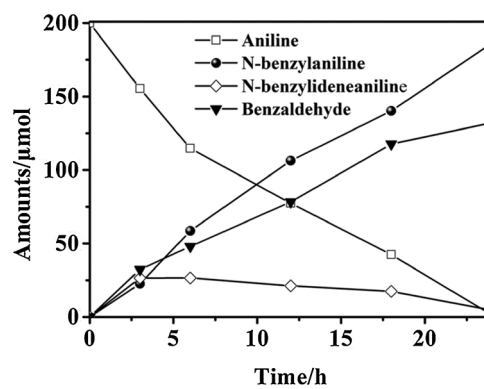


Fig. 6. Time-dependent changes in the amounts of aniline and the three products during N-alkylation of aniline with benzyl alcohol under visible-light irradiation over 0.5 wt% Pd-ZnIn₂S₄.

electron-rich Pd to generate Pd hydride (step 3). Similar light induced oxidant-free production of benzaldehyde from the dehydrogenation of benzyl alcohol has been documented previously [39,40]. The condensation between the in-situ generated benzaldehyde and the aniline can be promoted by the Lewis acidic sites in Pd-ZnIn₂S₄ to produce 3b as the intermediate (step 4). Finally a further hydrogenation of 3b catalyzed by the active Pd hydride generates N-alkylating product 3a (step 5).

An efficient N-alkylation of aniline can be realized by synchronizing the rates of the above tandem/cascade steps. In the N-alkylation of aniline reaction, the rate for photocatalytic dehydrogenation of benzyl alcohol depends on ZnIn₂S₄ based photocatalysis, which can be influenced by the deposited Pd nanoparticles since Pd nanoparticles are good electron traps and can help to promote the separation of the photogenerated charge carriers in ZnIn₂S₄. In addition, the cleavage of C–H bond in alkoxide intermediate promoted by Pd nanoparticles is important for the formation of benzaldehyde [19]. Moreover, the hydrogenation of the intermediate 3b, which formed via the condensation between benzaldehyde and aniline, is catalyzed by the active Pd hydride. Therefore, by varying the amount of deposited Pd and modifying its existing state, it is possible to tune the reaction rates of different steps to optimize the whole N-alkylation reaction. Actually, it was found that although the conversion of aniline remains almost unchanged (84%) when the amount of Pd was decreased to 0.3 wt%, the yield to the desired alkylation product 3a decreased from 73% to 51%, implying a lower of the rate for the hydrogenation of 3b to produce 3a (Table 1, entry 13). However, when the amount of Pd was increased to 1.0 wt%, both the conversion of aniline (69%) and the production of benzaldehyde (74 μmol) decreased slightly as compared with those in 0.5 wt% Pd-ZnIn₂S₄ (82% and 93 μmol respectively), probably due to a shading effect since the deposited Pd nanoparticles would cover the active site of ZnIn₂S₄ (Table 1, entry 14). In addition, 0.5 wt% Pd/ZnIn₂S₄ obtained via a chemical reduction process using NaBH₄ as reducing agent was also used for N-alkylation of aniline reaction. The TEM and HRTEM images of 0.5 wt% Pd/ZnIn₂S₄ show larger Pd nanoparticles of ca. 8.0 nm are deposited on ZnIn₂S₄ microspheres (Supporting information Fig. S3). Although chemical reduced 0.5 wt%Pd-ZnIn₂S₄ show a comparable conversion of aniline (78%), the yield to the desired alkylation product 3a is lower (55%) as compared with that over photo-reduced 0.5 wt% Pd-ZnIn₂S₄ (Table 1 entry 15). The higher selectivity to the desired N-alkylation product 3a over 0.5 wt% Pd-ZnIn₂S₄ may be ascribed to the smaller Pd nanoparticles, which contain more active unsaturated Pd atoms than those obtained via NaBH₄ reduction.

The N-alkylation of amines with alcohols to generate N-alkylated amines over 0.5 wt% Pd-ZnIn₂S₄ nanocomposites can also be applied to a wide substrate scopes (Table 2). Different functional group substituted anilines can be transformed to the corresponding N-alkyl anilines, but with different yields. As compare with bare aniline, anilines with electron-withdrawing groups such as *p*-Cl exhibited obviously increased yield to targeted N-alkyl amine (99%), while aniline with electron-donating substituents, such as *p*-OCH₃ or *p*-CH₃, showed decreased yields to N-alkyl amines (20–71%) (Table 2, entries 1–3), suggesting the existence of an electronic effect. Similarly, the reactions between benzyl alcohols with different substituents and aniline proceeded with medium to high conversion ratios of aniline (45–82%) and reasonable yields of N-alkyl amines (26–81%) after irradiation for 18 h over 0.5 wt% Pd-ZnIn₂S₄ nanocomposites (Table 2, entries 5–7). The scope of the substrates can also be expanded to a wide range of amines as well as aliphatic alcohols, although lower performance is observed over the later (Table 2, entries 8–13).

Since the alkylation of α-H of ketones with alcohols also proceeds via a similar hydrogen auto-transfer mechanism [41–44], Pd-ZnIn₂S₄ nanocomposites were also applied for the alkylation of α-H of ketone. The reaction between the benzyl alcohol and acetophenone (7a) was chosen as a model reaction. It was found that the α-H alkylated product

Table 2

Light induced catalytic performance for N-alkylation of different amines with alcohols over 0.5 wt% Pd-ZnIn₂S₄.

Entry	Substrates		Amine conv. /%	Yield /% 6a	Aldehydes /μmol 6b
	4a	5a			
1	benzyl alcohol	<i>p</i> -Methylaniline	99	71	26
2	benzyl alcohol	<i>p</i> -Methoxyaniline	51	20	30
3	benzyl alcohol	<i>p</i> -Chloroaniline	99	99	< 1
4	benzyl alcohol	<i>m</i> -Chloroaniline	98	94	4
5 ^a	<i>p</i> -Methylbenzyl alcohol	aniline	63	38	25
6 ^a	<i>p</i> -Methoxybenzyl alcohol	aniline	45	26	17
7 ^a	<i>p</i> -Chlorobenzyl alcohol	aniline	82	81	< 1
8	benzyl alcohol	Octylamine	35	16	15
9	benzyl alcohol	<i>n</i> -Butylamine	99	89	8
10	benzyl alcohol	cyclohexylamine	99	82	14
11	benzyl alcohol	furfurylamine	66	27	33
12	phenylethanol	aniline	15	6	8
13	furfuralcohol	aniline	23	12	9

Reaction conditions: amine (0.2 mmol), 0.5 wt% Pd-ZnIn₂S₄ (10 mg), CH₃CN (0.2 mL), alcohols (1.8 mL), N₂, irradiated for 18 h. ^a the solvent (2 mL) CH₃CN containing excess alcohols.

^b refers to no products or negligible products detected.

3-phenylpropiophenone (8a) was obtained with intermediates chalcone (8b) and benzaldehyde as the main byproducts. Both bases and the reaction medium influenced the catalytic performance. Especially, since base can promote the dehydrogenation of ketones' α-H to form enolate, the base influences significantly the conversion of the ketone and the yield to the targeted alkylated product (Table 3, entries 1–9). An optimum performance with a conversion of acetophenone at 81% and a yield of 71% to 8a was obtained when the reaction was carried out in a

Table 3

Light induced catalytic performance for α-H alkylation of acetophenone with different alcohols over 0.5 wt% Pd-ZnIn₂S₄.

Entry	Solvent	Base	Acetophenone Conv. /%	Yield /%		Aldehyde /μmol
				8a	8b	
1	phenyl alcohol	Cs ₂ CO ₃	56	43	12	78
2	phenyl alcohol	K ₂ CO ₃	38	22	11	56
3	phenyl alcohol	Na ₂ CO ₃	16	4	12	32
4	phenyl alcohol/ CH ₃ CN (4:1)	Cs ₂ CO ₃	71	49	16	75
5	phenyl alcohol/ toluene (4:1)	Cs ₂ CO ₃	40	15	18	45
6	phenyl alcohol/ ethanol (4:1)	Cs ₂ CO ₃	81	71	8	91
7	phenyl alcohol/ ethanol (2:1)	Cs ₂ CO ₃	56	36	17	67
8	phenyl alcohol/ ethanol (1:2)	Cs ₂ CO ₃	66	35	29	74
9	phenyl alcohol/ ethanol (1:4)	Cs ₂ CO ₃	50	24	13	55
10	phenylethanol/ ethanol (4:1)	Cs ₂ CO ₃	3	0.9	2	6
11	furfuralcohol/ ethanol (4:1)	Cs ₂ CO ₃	10	4	6	13

Reaction conditions: acetophenone (0.2 mmol), catalyst (10 mg), solvent (2.0 mL), base (0.1 mmol), N₂, irradiated for 24 h.

mixed solvent containing benzyl alcohol and ethanol in a volume ratio of 4:1 with the presence of Cs_2CO_3 (Table 3, entry 6). This reaction can also be expanded to aliphatic alcohols, like furfuralcohol and phenylethanol, although with a low conversion (Table 3, entries 10–11).

4. Conclusion

In summary, Pd-ZnIn₂S₄ nanocomposites with small Pd nanoparticles of an average size of 6.0 nm were successfully obtained via photoreduction of $\text{Pd}(\text{CH}_3\text{CN})_2\text{Cl}_2$ over ZnIn₂S₄ and were used for visible light induced alkylation of amines and α -H of ketones with alcohols to construct C–N and C–C bonds. By synchronization of the rates of different reaction steps in the tandem alkylation reaction, an optimum performance was realized over 0.5 wt% Pd-ZnIn₂S₄. Ascribable to the small sized Pd nanoparticles to provide more unsaturated active unsaturated Pd atoms, 0.5 wt% Pd-ZnIn₂S₄ show superior performance as compared to 0.5 wt% Pd/ZnIn₂S₄ obtained via a chemical reduction using NaBH₄. This study provides an efficient way to realize a highly efficient and stable alkylation of amines and α -H of ketones via a successful coupling of the visible light semiconductor-based photocatalysis and Pd NPs-based hydrogenation. This study also highlights the great potential of construction of multifunctional photocatalysts for light induced organic syntheses.

Acknowledgements

This work was supported by NSFC (U1705251) and 973 Program (2014CB239303). Z. Li thanks the Award Program for Minjiang Scholar Professorship for financial support.

Appendix A. Supplementary data

Supplementary material related to this article can be found, in the online version, at doi:<https://doi.org/10.1016/j.apcatb.2018.06.067>.

References

- [1] G. Guillena, J. R. D and M. Yus, Chem. Rev., 110 (2010) 1611–1641.
- [2] D. Ma, A. Liu, S. Li, C. Liu, C. Chen, Catal. Sci. Technol. 8 (2018) 2030–2045.
- [3] C.S. Yeung, V.M. Dong, Chem. Rev. 111 (2011) 1215–1292.
- [4] T.T. Dang, B. Ramalingam, S.P. Shan, A.M. Seayad, ACS Catal. 3 (2013) 2536–2540.
- [5] Y. Watanabe, Y. Tsuji, Y. Ohsugi, Tetrahedron Lett. 22 (1981) 2667–2670.
- [6] R. Grigg, T.R.B. Mitchell, S. Sutthivaiyakit, N. Tongpenyai, J. Chem. Soc. Chem. Commun. (1981) 611–612.
- [7] M.H.S.A. Hamid, C.L. Allen, G.W. Lamb, A.C. Maxwell, H.C. Maytum, A.J.A. Watson, J.M.J. Williams, J. Am. Chem. Soc. 131 (2009) 1766–1774.
- [8] S. Rosler, M. Ertl, T. Irrgang, R. Kempe, Angew. Chem. Int. Ed. 54 (2015) 15046–15050.
- [9] H. Liu, G.-K. Chuah, S. Jaenicke, J. Catal. 292 (2012) 130–137.
- [10] M.M. Reddy, M.A. Kumar, P. Swamy, M. Naresh, K. Srujana, L. Satyanarayana, A. Venugopal, N. Narendra, Green. Chem. 15 (2013) 3474–3483.
- [11] J.W. Kim, K. Yamaguchi, N. Mizuno, J. Catal. 263 (2009) 205–208.
- [12] K. Shimizu, R. Sato, A. Satsuma, Angew. Chem. Int. Ed. 48 (2009) 3982–3986.
- [13] Y. Zhao, S.W. Foo, S. Saito, Angew. Chem. Int. Ed. 50 (2011) 3006–3009.
- [14] X. Lang, X. Chen, J. Zhao, Chem. Soc. Rev. 43 (2014) 473–486.
- [15] A. Dhakshinamoorthy, A.M. Asiri, H. Garcia, Angew. Chem. Int. Ed. 55 (2016) 5414–5445.
- [16] X. Lang, H. Ji, C. Chen, W. Ma, J. Zhao, Angew. Chem. Int. Ed. 50 (2011) 3934–3937.
- [17] L. Deng, Li Z, H. Garcia, Chem. Eur. J. 23 (2017) 11189–11209.
- [18] D. Ma, Y. Yan, H. Ji, C. Chen, J. Zhao, Chem. Commun. 50 (2015) 17451–17454.
- [19] Y. Shiraishi, K. Fujiwara, Y. Sugano, S. Ichikawa, T. Hirai, ACS Catal. 3 (2013) 312–320.
- [20] L. Zhang, Y. Zhang, Y. Deng, F. Shi, RSC Adv. 5 (2015) 14514–14521.
- [21] D. Stibal, J. Sá, J. Av. Bokhoven, Catal. Sci. Technol. 3 (2013) 94–98.
- [22] L. Zhang, Y. Zhang, Y. Deng, F. Shi, Catal. Sci. Technol. 5 (2015) 3226–3234.
- [23] D. Wang, Z. Li, J. Catal. 342 (2016) 151–157.
- [24] D. Wang, Y. Pan, L. Xu, Z. Li, J. Catal. 361 (2018) 248–254.
- [25] L. Ye, J. Fu, Z. Xu, R. Yuan, Z. Li, ACS Appl. Mater. Interfaces 6 (2014) 3483–3490.
- [26] L. Wei, Y. Chen, Y. Lin, H. Wu, R. Yuan, Z. Li, Appl. Catal. B: Environ. 144 (2014) 521–527.
- [27] L. Shang, C. Zhou, T. Bian, H. Yu, L.-Z. Wu, C.-H. Tung, T. Zhang, J. Mater. Chem. A 1 (2013) 4552–4558.
- [28] S. Shen, L. Zhao, Z. Zhou, L. Guo, J. Phys. Chem. C 112 (2008) 16148–16155.
- [29] Y. Chen, S. Hu, W. Liu, X. Chen, L. Wu, X. Wang, P. Liu, Z. Li, Dalton Trans. 40 (2011) 2607–2613.
- [30] G. Mamba, A.K. Mishra, Appl. Catal. B: Environ. 198 (2016) 347–377.
- [31] M. Wang, L. Li, J. Lu, N. Luo, X. Zhang, F. Wang, Green. Chem. 19 (2017) 5172–5177.
- [32] L. Su, X. Ye, S. Meng, X. Fu, S. Chen, Appl. Surf. Sci. 384 (2016) 161–174.
- [33] L. Ye, Z. Li, ChemCatChem 6 (2014) 2540–2543.
- [34] H.T. Luu, S. Wiesler, G. Frey, J. Streuff, Org. Lett. 17 (2015) 2478–2481.
- [35] Y. Zhao, X. Yang, J. Tian, F. Wang, L. Zhan, Int. J. Hydrogen Energy 35 (2010) 3249–3257.
- [36] L. Ye, Z. Li, Appl. Catal. B: Environ. 160–161 (2014) 552–557.
- [37] Y. Chen, R. Huang, D. Chen, Y. Wang, W. Liu, X. Li, Z. Li, ACS Appl. Mater. Interfaces 4 (2012) 2273–2279.
- [38] Y. Guo, L. Xiao, M. Zhang, Q. Li, J. Yang, Appl. Surf. Sci. 440 (2018) 432–439.
- [39] W. Fang, J. Chen, Q. Zhang, W. Deng, Y. Wang, Chem. Eur. J. 17 (2011) 1247–1256.
- [40] D. Ma, A. Liu, C. Lu, C. Chen, ACS Omega 2 (2017) 4161–4172.
- [41] S. Bhat, V. Sridharan, Chem. Commun. 48 (2012) 4701–4703.
- [42] M. Dixit, M. Mishra, P.A. Joshi, D.O. Shah, Catal. Commun. 33 (2013) 80–83.
- [43] K. Shimura, K. Kon, S.M.A. Hakim Siddiki, K.-i. Shimizu, Appl. Catal. A: Gen. 462–463 (2013) 137–142.
- [44] R. Cano, M. Yus, D.J. Ramon, Chem. Commun. 48 (2012) 7628–7630.